Electronic Full-Space Scanning With 1D Fabry-Pérot LWA Using Electromagnetic Band Gap

Raúl Guzmán-Quirós, *Student Member, IEEE*, José Luis Gómez-Tornero, *Member, IEEE*, Andrew R. Weily, *Member, IEEE*, and Y. Jay Guo, *Senior Member, IEEE*

***Abstract*— A novel mechanism to obtain full-space electronic scanning from a half-space scanning one-dimensional (1D) Fabry-Pérot (FP) leaky-wave antenna (LWA) is proposed and experimentally demonstrated in this letter. By using a central feed which divides the structure in two independently controlled leaky lines one each side, and making use of the electromagnetic band gap (EBG) region of the FP resonator, the antenna can be electronically tuned to operate in three different regimes: backward scanning, forward scanning, and broadside radiation. Leaky-mode dispersion theory and experimental results of a fabricated prototype demonstrate a continuous electronic scanning from -25° to +25° at 5.5 GHz.**

***Index Terms*— Leaky-wave antenna (LWA), electronic beam scanning, Fabry-Pérot antenna, electromagnetic band gap.**

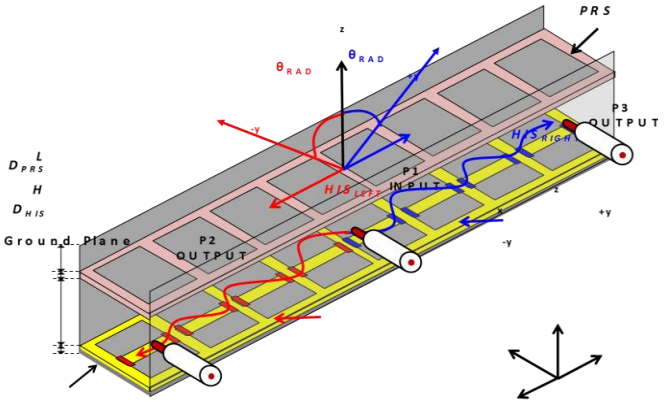

Fig.1. Scheme of the proposed full-space scanning 1D FP LWA.

I. Introduction

FULL-SPACE electronic scanning is a desirable feature for leaky-wave antennas (LWAs), since it allows at a fixed frequency to steer the beam from negative to positive angles, including the broadside direction. This has been achieved by inserting active components in different one-dimensional (1D) LWA technologies, such as composite right/left handed (CRLH) microstrip [1,2], textured high-impedance surfaces [3], half-width microstrip [4], or CRLH half-mode substrate-integrated technology [5]. Full-space scanning is more complicated than half-space steering, requiring more independently controlled diodes/switches to generate backward-to-forward leaky waves [3,4], and very demanding design constraints to control the CRLH over the complete angular region [6]. For this reason, a simpler end-switched topology has been recently proposed in [6], which makes use of a two-port half-space scanning CRLH LWA and a single-pole double-throw (SPDT) switch. In this way, only half-space electronic control is needed and the design constraints are strongly simplified.

In this letter we demonstrate a novel topology to provide full-space scanning by using a half-space scanning 1D LWA in Fabry-Pérot (FP) technology, which was recently proposed by the authors in [7]. This full-scanning topology is simpler than [6] as only one input port is needed, thus avoiding the use of routing switches and associated control signals. Section II theoretically describes the proposed new mechanism to obtain full-space steering, while experimental results are reported in Section III. An important advantage of the proposed 1D FP configuration is the natural extension to 2D steerable FP antennas [8,9] which is described in the conclusions.

II. Full-Space Scanning using 1D Fabry-Pérot LWA

A scheme of the proposed configuration is illustrated in Fig.1. In [7] it was shown how a 1D FP LWA can be loaded with a tunable high impedance surface (HIS) to obtain half-space electronic beam steering from +9º to +30º. The input port of the steerable LWA in [7] was located at one end of the 1D FP leaky waveguide. This original structure is modified here by locating the input port in the middle point (P1 in Fig.1), and by using two independently tuned HIS located at each side of the center feeding (HIS_{LEFT} and HIS_{RIGHT} in Fig.1).

Two leaky waves propagating in opposite directions (+y and –y in Fig.1) will be launched by the central feed, each one being controlled by the corresponding HIS. This control is illustrated in Fig.2, which plots the dispersion of the leaky-mode complex propagation constant as a function of the HIS varactors' junction capacitance (C_j), at the fixed design frequency of 5.5GHz (the dimensions of the FP LWA are described in detail in [7]). Results obtained with the Transverse Resonance Method (TRM) employed in [7] and HFSS simulations are in good agreement, observing two well differentiated regions:

i) A scanning region where the leaky-wave phase constant is varied from $\beta_y/k_0 \approx 0.1$ ($\theta_{RAD} \approx 6º$) for $C_j = 0pF$ to $\beta_y/k_0 \approx 0.9$ ($\theta_{RAD} \approx 64º$) for $C_j = 0.27pF$, thus providing half-space steering.

ii) An electromagnetic band-gap (EBG) region for $C_j = [0.27pF, 0.3pF]$, for which propagation of the leaky mode along the FP waveguide is prevented, as shown by the strong rise of the attenuation constant α_y/k_0 and the null value of $d\beta_y/dC_j$.

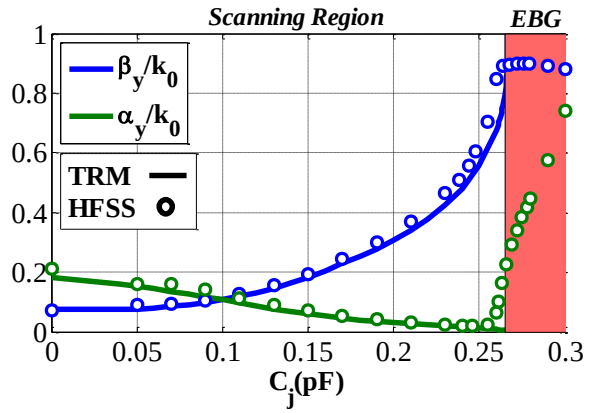

Fig.2. Effect of C_j on the leaky-mode dispersion for the half-space scanning 1D FP LWA at 5.5GHz.

This EBG regime can be used to route the input signal to the right or left directions. In this way three operation regimes are proposed to obtain full-space electronic scanning:

1) Backward scanning regime. To scan at negative angles, HIS_{LEFT} must be tuned inside the scanning region ($C_{jL} < 0.27pF$) while HIS_{RIGHT} is fixed at EBG region ($C_{jR} = 0.3pF$). In this way the input signal is guided to the left side of the LWA and no energy travels to the right side, as it can be seen in Fig.3-a. By properly tuning C_{jL} in the range [0pF,0.27pF], a single beam pointing at negative angle should be theoretically scanned in the angular region $\theta_{RAD} = [-6º, -64º]$.

2) Forward scanning regime. This is the symmetrical case, as shown in Fig.3-b. HIS_{LEFT} is operated in the EBG regime

(C_{jL}=0.3pF) and HIS$_{RIGHT}$ is tuned in the scanning region to provide steering at positive angles (with C_{jR}=[0pF,0.27pF] to theoretically obtain θ_{RAD}=[+6°,+64°]).

3) Broadside radiation. Optimum radiation at boresight can be obtained by launching two opposite-directed leaky waves which satisfy the splitting condition $\beta_y/k_0=\alpha_y/k_0$ [10]. To this end, HIS$_{LEFT}$ and HIS$_{RIGHT}$ are tuned at the same operating point inside the scanning region with $C_{jR}=C_{jL}$=0.1pF, which satisfies this splitting condition according to Fig.2. Fig.3-c illustrates this case, showing how the fields on the two sides of the antenna merge to form a single beam radiating at θ_{RAD}=0°.

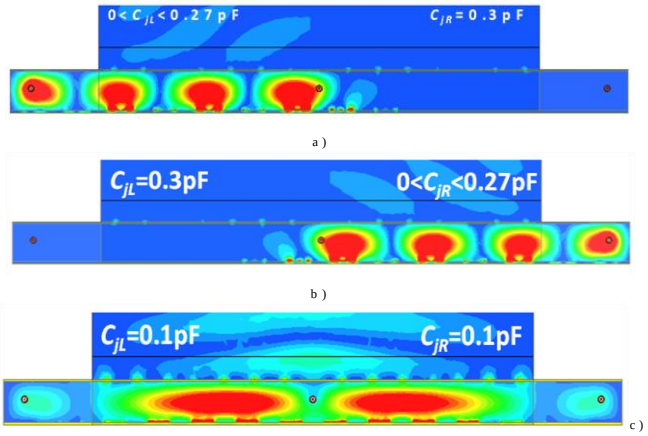

Fig.3. HFSS field distribution along the antenna for the three operating regimes: a) Backward scanning b) Forward scanning, c) Broadside radiation.

III. Experimental Results

A prototype of the proposed full-space scanning 1D FP LWA has been fabricated as shown in Fig.4, where the coaxial input port located at the center (P1) and the two output ports at each side (P2 and P3) are shown. Fig.4 also shows the cables that supply voltages to the two independently controlled HIS$_{LEFT}$ and HIS$_{RIGHT}$, respectively biased with DC voltages V_L and V_R, and a detailed photograph of a tunable HIS unit cell including its biasing network.

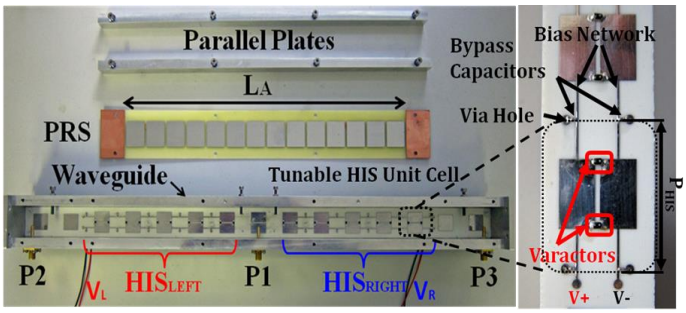

Fig.4. Manufactured full-space scanning 1D FP LWA prototype ($L_A = 5\lambda_0$).

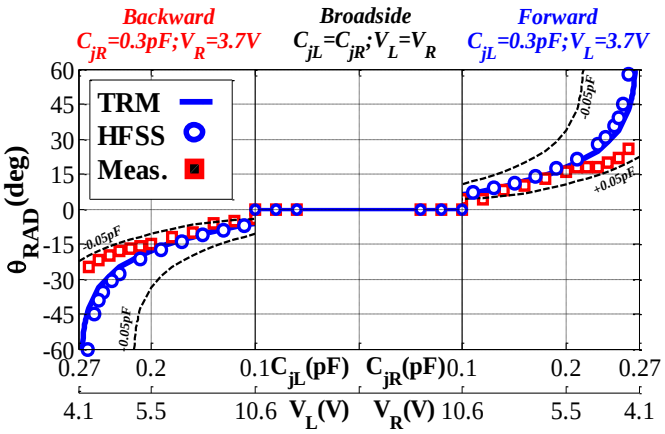

Fig.5. Measured and simulated scanning response for the full-space scanned 1D FP LWA at 5.5GHz.

The theoretical and measured scanning response at 5.5GHz is plotted in Fig.5, showing the variation of the pointing angle θ_{RAD} as a function of the varactor junction capacitance C_j (for theoretical results obtained with TRM and HFSS), and as a function of the bias voltage V (for experiments). As explained in [7], the correspondence between C_j and V in this double-x-axis is obtained with a calibration of the varactors. It is important to notice that this double x-axis in Fig.5 is divided into three regions which correspond to the three aforementioned operation regimes of the electronically controlled FP LWA. The left side of Fig.5 represents the backward scanning configuration, for which HIS_{RIGHT} is biased with fixed V_R=3.7V (corresponding to C_{jR}=0.3pF for EBG operation), while HIS_{LEFT} is controlled with V_L varying in the range [4.1V,10.6V] (which corresponds to C_{jL}=[0.27pF,0.1pF] to operate in the scanning region). The symmetrical biasing configuration is represented in the right side of Fig.5, showing a fixed value of V_L=3.7V and C_{jL}=0.3pF (HIS_{LEFT} at EBG) and varying V_R=[4.1V,10.6V] and C_{jR}=[0.27pF,0.1pF] to obtain forward scanning.

Finally, the central section in Fig.5 represents the broadside configuration, for which symmetrical biasing is applied with V_L=V_R=[10.6V,18V] and C_{jL}=C_{jR}=[0.1pF,0.06pF]. Very good agreement is observed for the theoretical scanning response obtained with TRM and commercial HFSS software, obtaining a scanning range of θ_{RAD}=[-60°,+60°]. Experimental results are plotted with red rectangles, showing good matching with theory for the angular region [-15°,+15°], but limiting the measured scanning range to [-25°,+25°]. These discrepancies can be attributed to the varactors tolerances, as explained in

[7]. Actually, the measured scanning response lies inside the theoretical scanning response obtained when applying a deviation of ±0.05pF to the junction capacitance C_j, as shown with dashed lines in Fig.5. Nevertheless, Fig.5 demonstrates that a backward-to-forward electronic scanning (including broadside radiation) can be obtained by using the proposed full-scanning configuration for FP LWAs.

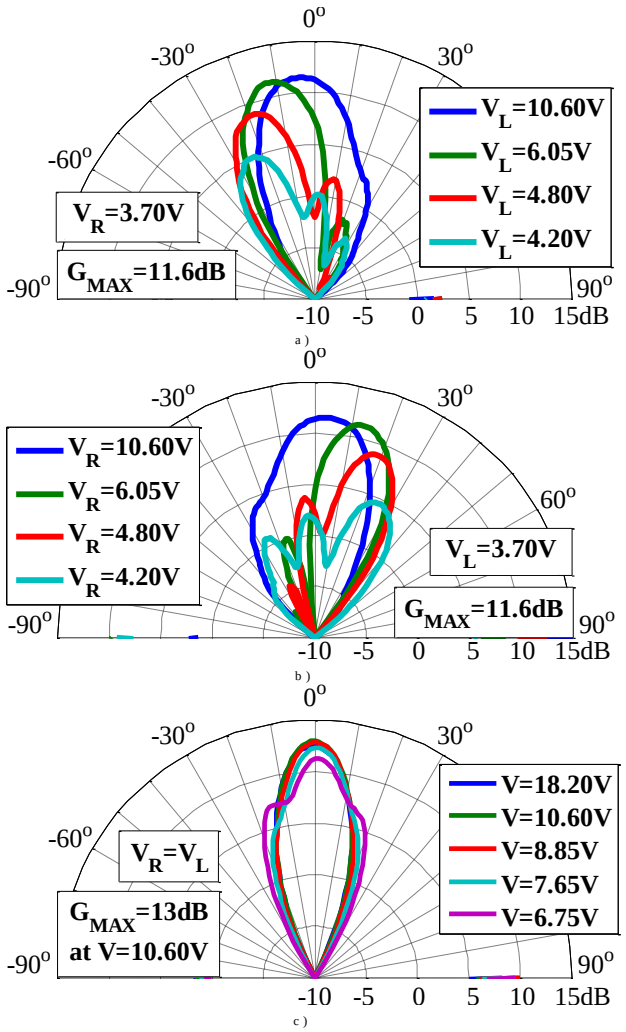

Fig.6. Measured gain patterns for the full-space scanned 1D FP LWA at 5.5GHz for the three operating configurations.

The measured gain patterns of the fabricated antenna operating at backward, forward, and broadside configurations are plotted in Fig.6. Fig.6-a illustrates the electronic scanning

at negative angles, showing a single main beam scanned from θ_{RAD}=-25° to θ_{RAD}=-5° as HIS$_{LEFT}$ is tuned from V_L=4.2V (C_j=0.26pF) to V_L=10.6V (C_j=0.1pF), while HIS$_{RIGHT}$ is fixed at V_R=3.7V (C_j=0.3pF). In Fig.6-b, the scanning response at positive angles is shown, observing a symmetrical steering from θ_{RAD}=+5° to θ_{RAD}=+25° by controlling HIS$_{RIGHT}$ between V_R=10.6V and V_R=4.2V and keeping HIS$_{LEFT}$ at V_L=3.7V. Both scanning regimes present a maximum gain of G_{max}=11.6dB for θ_{RAD}=±5°. However, slight asymmetries can be observed between the scanning responses for the negative and positive quadrants: this is most likely due to manufacturing tolerances and variation in the performance of the varactor diodes for each HIS circuit. In particular, higher side lobes can be seen when scanning toward forward endfire than towards backward endfire, resulting in gain values of G=5dB for θ_{RAD}=-25° and G=4.5dB for θ_{RAD}=+25°. This gain fall as the pointing angle is scanned is due to several loss factors such as the leakage rate drop, dielectric and varactor dissipation and mismatch, as explained in [7]. Nevertheless, the concept of using the EBG regime of the FP leaky line to guide the input energy to the desired quadrant is experimentally demonstrated, resulting in a main beam scanned in the corresponding radiation quadrant while preventing radiation in the opposite direction.

Fig.6-c is dedicated to the broadside radiation operation. As described before, the same bias voltage must be applied to both HIS circuits, V_L=V_R. Particularly, the splitting condition is satisfied for V=10.6V (which theoretically corresponds to C_j=0.1pF where β_y/k_0=α_y/k_0 in Fig.2), obtaining a single beam radiating at broadside with maximum gain G_{max}=13dB. Moreover, it is shown that the voltage can be varied in the range V=[18.2V,6.75V], and still a single beam at boresight is obtained. However, the gain decreases and side lobes start to appear as we move further from the splitting condition [10], as it can be seen in Fig.6-c for V=6.75V (which corresponds to C_j=0.16pF, where β_y/k_0=0.2>α_y/k_0=0.05 in Fig.2), which provides lower gain at broadside G=11.3dB. Thus, it is experimentally checked that optimum radiation at broadside is obtained when both HIS are tuned at the splitting condition. The radiation patterns in Fig.6 experimentally demonstrate backward-to-forward electronic scanning of the proposed FP antenna. It must be noticed that only half of the antenna aperture is effectively used when operating in either backward or forward scanning regimes, thus obtaining a wider main beam and lower gain compared to broadside operation (in which most of the antenna aperture is radiating, see Fig.3).

Fig.7-a shows the input matching of the full-space scanning FP LWA as a function of the biasing voltage V (and corresponding C_j) at the fixed design frequency of 5.5GHz. The matching circuit makes use of tuning screws (which can be seen in Fig.4), which were optimized to provide low S_{11} for most of the scanning range including broadside. The antenna presents S_{11}≈-8dB in the broadside radiation configuration, while in the backward and forward scanning regimes the mismatch increases from -15dB to -5dB as the beam is steered towards endfire. Similar tendency is observed with HFSS simulations and measurements. Some asymmetry between backward/forward scanning is again observed in measured S_{11}. It is worthy to note that matching of the full-space scanning

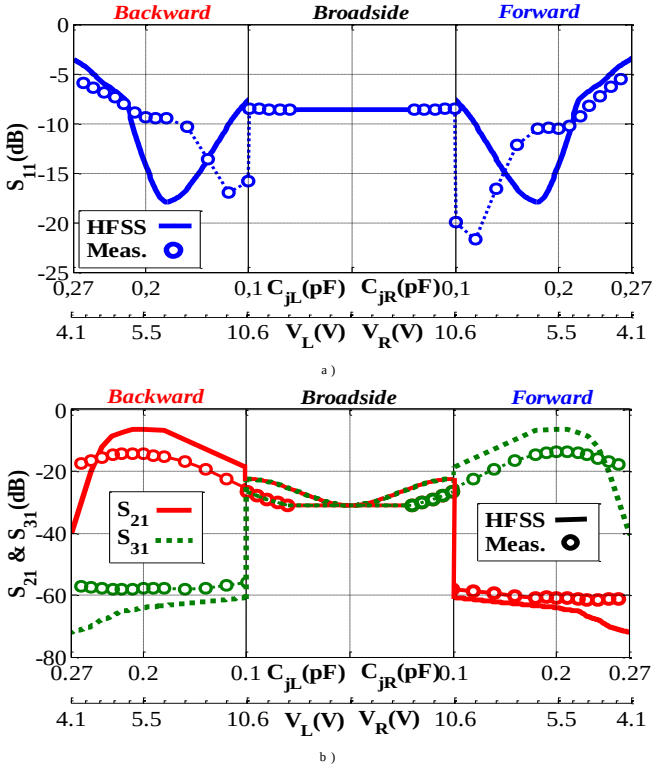

Fig.7. Measured and simulated S-parameters for the full-space scanned 1D FP LWA at 5.5GHz. a) Input matching S_{11} b) Transmission S_{21}, S_{31}.

FP LWA is more difficult than its half-space counterpart [7] because it operates in three different scanning regimes, with dramatic changes in the leaky mode field distribution. As a result, matching is worse than in the half-space design.

Fig.7-b illustrates the transmission coefficients between the input port and the two ports located at the left (S_{21}) and right (S_{31}) sides (see Fig.4). As expected, when the antenna is operated in the backward scanning regime, the leaky wave is guided to the left side resulting in very low $S_{31}\approx$-60dB (due to the EBG regime provided by HIS_{RIGHT}) and $S_{21}\approx$-20dB (which corresponds to the energy which has not been radiated by the left-propagating leaky wave, see Fig.3-a). These values are interchanged in the forward-scanning configuration, showing $S_{21}\approx$-60dB and $S_{31}\approx$-20dB, since the energy is guided to the right side. Finally, in the broadside regime the energy is guided to both sides presenting equal values of $S_{21}=S_{31}\approx$-30dB. The transmission at broadside is 10dB lower than in the scanning configuration due to the fact that leaky wave presents higher leakage rate at the broadside splitting condition ($\alpha_y/k_0>0.1$) than for higher scanning angles $\alpha_y/k_0<0.1$ as shown in Fig.2). Good agreement between experiments and simulations is observed for the transmission coefficients in the three regimes, confirming the ability of the proposed FP LWA to route the leaky-wave to the desired direction.

IV. Conclusion

A novel topology to obtain electronic full-space scanning from a 1D Fabry-Pérot (FP) LWA has been described and experimentally demonstrated. The full-space is scanned by virtue of the EBG properties of the FP, which routes the signal to the desired half-space scanning antenna. In this way, the switching mechanism proposed in [6] which needs a SPDT switch and associated control signals is avoided. It should be pointed out that the proposed EBG routing mechanism is less efficient than [6], as only 50% of the antenna aperture is used to scan the beam in each quadrant. Nevertheless, the main advantage of this EBG routing proposal compared to switching schemes is that it can be naturally extended to 2D FP LWA, as illustrated with an example in Fig.8. A 2D FP antenna is divided in several discrete sectors (S1-S4) which are independently tuned, so that the leaky wave excited at the center of the FP cavity can be routed to any of these sectors by tuning the others to EBG regime. In this way, discrete azimuthal sectorization could be obtained, providing 2D scanning of a pencil beam (in elevation θ and azimuthal ϕ angles) in contrast to scanned conical beams [8], and without using phased-arrays [9]. However, it must be noticed that only 25% of the antenna aperture would be illuminated, except for the broadside radiation case.

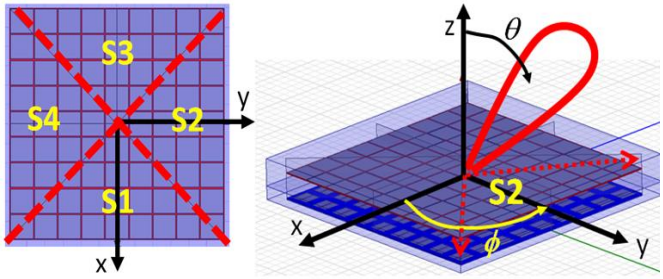

Fig.8. Extension of the EBG routing mechanism for full-space 2D electronic scanning in Fabry-Pérot antennas.

References

[1] S. Lim, C. Caloz, and T. Itoh, "Electronically scanned composite right/left handed microstrip leaky-wave antenna," *IEEE Microwave and Wireless Components Lett.*, vol.14, no.6, pp. 277-279, June 2004.

[2] S. Lim, C. Caloz, and T. Itoh, "Metamaterial-based electronically controlled transmission-line structure as a novel leaky-wave antenna with tunable radiation angle and beamwidth", *IEEE Trans. Microwave Theory and Techn.*, vol.52, no.12, pp. 2678-2690, Dec. 2004.

[3] D.F. Sievenpiper, "Forward and backward leaky wave radiation with large effective aperture from an electronically tunable textured surface," *IEEE Trans. Antennas Propag.*, vol. 53, no. 1, pp. 236-247 Jan. 2005.

[4] R.O. Ouedraogo, E.J. Rothwell, and B.J. Greetis, "A reconfigurable microstrip leaky-wave antenna with a broadly steerable beam," *IEEE Trans. Antennas Propag.*, vol.59, no.8, pp.3080-3083, Aug. 2011.

[5] A. Suntives, and S.V Hum, "A fixed-frequency beam-steerable half-mode substrate integrated waveguide leaky-wave antenna," *IEEE Trans. Antennas Propag.*, vol.60, no.5, pp.2540-2544, May 2012.

[6] H.V. Nguyen, S. Abielmona, and C. Caloz, "Performance-enhanced and symmetric full-space scanning end-switched CRLH LWA," *IEEE Antennas Wireless Propag. Lett.* vol.10, pp.709-712, 2011.

[7] R. Guzmán-Quirós, J.L. Gómez-Tornero, A.R. Weily, and Y. Jay Guo, "Electronically steerable 1D Fabry-Perot leaky-wave antenna employing a tunable high impedance surface," *IEEE Trans. Antennas Propag.*, vol. 60, no. 11, pp. 5046-5055, Nov. 2012.

[8] F. Costa and A. Monorchio, "Design of subwavelength tunable and steerable Fabry-Perot/leaky-wave antennas," *Progress In Electromagnetics Research*, vol. 111, pp. 467-481, 2011.

[9] T. Debogovic, J. Bartolic, and J. Perruisseau-Carrier, "Array-fed partially reflective surface antenna with dynamic beamwidth control and beam-steering," *6th European Conference on Antennas and Propagation (EUCAP 2012)*, pp.3599-3603, 26-30 March 2012.

[10] G. Lovat, P. Burghignoli and D. R. Jackson, "Fundamental properties and optimization of broadside radiation from uniform leaky-wave antennas," *IEEE Trans. Antennas Propag.*, vol. 54, pp. 1442–1452, May 2006.